MAUSAM, **77**, 3 (July 2026), 865-878

MAUSAM

DOI: https://doi.org/10.54302/mausam.v77i3.7194
Homepage: https://mausamjournal.imd.gov.in/index.php/MAUSAM

UDC No.556.166:551.577

Hydrometeorological dynamics of monsoon floods on the Kaveri River, Southern India

PRAMODKUMAR S. HIRE[1], SMITA R. PAGARE[2] and ARCHANA D. PATIL[3*]

[1&2]HPT Arts and RYK Science College, Nashik - 422005 (India)

(Affiliated to Savitribai Phule Pune University, Pune - 411007)

[3]RNC Arts, JDB Commerce and NSC Science College, Nashik Road, Nashik - 422101 (India)

(Affiliated to Savitribai Phule Pune University, Pune - 411007)

(*Received 6 July 2025, Accepted 8 October 2024*)

***Corresponding author's email: archanapatil.geo@gmail.com**

सार – इस अध्ययन का उद्देश्य दक्षिण भारत की कावेरी नदी पर मानसूनी बाढ़ की जलमौसमविज्ञानी गतिकी (Hydrometeorological dynamics) की जांच करना है। इसमें अंतर-वार्षिक वर्षा परिवर्तनशीलता और बाढ़ के साथ इसके सहसंबंध का विश्लेषण, बाढ़-प्रेरित कम दबाव प्रणालियों (LPS) का लक्षण वर्णन, गहराई-क्षेत्र-अवधि (DAD) मूल्यांकन, वार्षिक वर्षा योग और बाढ़ आवृत्तियों के बीच संबंध का आकलन, बाढ़ से जुड़ी विसंगतियों की पहचान करने के लिए माध्य से सामान्यीकृत संचित विचलन (NADM) विधि का अनुप्रयोग, और बाढ़ गतिकी को नियंत्रित करने वाले अल नीनो दक्षिणी दोलन (ENSO) की घटनाओं और मानसूनी वर्षा के प्रतिरूपों के बीच अंतःक्रिया की जांच शामिल है। अध्ययन में दो जलविज्ञानी निगरानी स्टेशनों के लिए 45 वर्षीय वार्षिक अधिकतम श्रृंखला के साथ एक 121-वर्षीय वर्षा डेटासेट को नियोजित किया गया है, जो वर्षा परिवर्तनशीलता और बाढ़ गतिकी के दीर्घकालिक सांख्यिकीय विश्लेषण को सक्षम बनाता है। परिणाम बताते हैं कि बेसिन में अंतर-वार्षिक परिवर्तनशीलता मुख्य रूप से 1960 के दशक के बाद बाढ़ की आवृत्ति और परिमाण में उल्लेखनीय वृद्धि से अभिलक्षित है। इसके अलावा, पर्याप्त बाढ़ की घटनाएं औसत से अधिक वर्षा की अवधियों के साथ मेल खाती हैं, जो बाढ़ गतिकी को संशोधित करने में वर्षा की विसंगतियों की महत्वपूर्ण भूमिका को रेखांकित करती हैं। तीव्र LPS मुख्य रूप से बेसिन में, विशेष रूप से डेल्टा क्षेत्र में बड़ी बाढ़ लाते हैं। 23-25 जुलाई 1924 की घटना के DAD वक्र ने 1-दिन, 2-दिन और 3-दिन की अवधि के लिए बेसिन में वर्षा की उच्चतम औसत गहराई में योगदान दिया है। प्रमुख बाढ़ से जुड़ी सिनॉप्टिक स्थितियों के विश्लेषण से संकेत मिलता है कि अधिकांश बाढ़ बेसिन में औसत वर्षा से धनात्मक विचलन से जुड़ी थीं। NADM ग्राफ उच्च और निम्न वर्षा और इसलिए बाढ़ के युगीन व्यवहार (Epochal behaviour) को दर्शाते हैं। बाढ़ की आवृत्ति आमतौर पर सामान्य या कमजोर ENSO स्थितियों वाले वर्षों में अधिक होती है।

ABSTRACT. This study aims to investigate the hydrometeorological dynamics of monsoon floods on the Kaveri River, Southern India. It encompasses the analysis of interannual rainfall variability and its correlation with floods, characterization of flood-inducing low-pressure systems (LPS), depth-area-duration (DAD) evaluation, assessment of the relationship between annual rainfall totals and flood frequencies, application of the normalized accumulated departure from mean (NADM) method to identify flood-linked anomalies, and investigation of the interplay between El Niño southern oscillation (ENSO) phenomena and monsoon rainfall patterns governing flood dynamics. The study employs a 121-year rainfall dataset, coupled with a 45-year annual maximum series for two hydrological monitoring stations, enabling long-term statistical analysis of rainfall variability and flood dynamics. The results indicate that the interannual variability in the basin is characterized by a notable increase in the frequency and magnitude of floods, particularly post-1960s. Moreover, substantial flood events coincided with periods of above-average rainfall, underscoring the significant role of rainfall anomalies in modulating flood dynamics. Intense LPS predominantly drive major floods in the basin, especially in the deltaic zone. DAD curve of 23-25 July 1924 event has contributed the highest average depth of rainfall over the basin for 1-day, 2-day and 3-day duration. Analysis of synoptic conditions associated with major floods indicate

that most of the floods were associated with positive departure from mean rainfall in the basin. The NADM graphs show epochal behaviour of high and low rainfall and therefore, floods. The frequency of floods is generally high in years with normal or weak ENSO conditions.

Key words – Flood hydrometeorology, Monsoon, Floods, Kaveri river.

1. Introduction

In flood hydrometeorology, the spatiotemporal distribution and genesis of large-scale flood events are predominantly governed by episodes of intense to extreme rainfall, representing a critical focus of scientific inquiry. In general, the occurrence of floods is attributed to exceptional synoptic conditions that generate precipitation exceeding a drainage basin's capacity for absorption and storage (Hirschboeck, 1988). The majority of river floods are climatological phenomena, arising either directly from precipitation events or indirectly from the melting of snow and ice (Ward, 1978). This has led to a focused investigation of precipitation-generating processes across diverse spatial and temporal scales by meteorologists, climatologists and hydrologists. Hydrometeorology is commonly employed to investigate floods. However, from a broader perspective, insights gained from hydrometeorological research have been utilized to analyse flood variability over extended periods (Hirschboeck, 1988). In the Indian context, widespread flooding in major river basins results from the synergistic interaction of synoptic-scale monsoonal intensification, antecedent hydrometeorological conditions, and physiographic controls, all moderated by large-scale atmospheric moisture flux convergence and interannual climate variability (Nanditha and Mishra, 2024).

Early investigations into these dynamics within the present study area—the Kaveri (Cauvery) Basin, include Banerji and Narayanan's (1966) comprehensive hydrometeorological investigation, which encompassed major flood episodes between 1892 and 1956 as well as the significant 1961 event. Their analysis revealed that most floods were linked to intensified monsoon activity, predominantly triggered by synoptic-scale depressions over the Bay of Bengal, underscoring a strong atmospheric–fluvial coupling in flood genesis. Subsequent work by Sawant, *et al*. (2015) analysed spatio-temporal rainfall variability over the Kaveri Basin during the twentieth century, while Sreelash, *et al*. (2020) assessed recent alterations in the hydrological regime and examined the links between shifting rainfall patterns and their impacts on the hydrological characteristics of the Kaveri Basin. The study reported significant declines in both total precipitation and the frequency of rainfall events, particularly across the middle basin, which manifested as reduced streamflows in the main stem and tributaries and highlighted the basin's pronounced sensitivity to ongoing climatic variability.

Building on these earlier assessments and recognizing the paucity of research on monsoon flood hydrometeorology in the Kaveri Basin, the present study undertakes a comprehensive analysis of the synoptic conditions associated with large-scale flood events. It explores interannual rainfall variability in relation to flood occurrences, applies the Normalized Accumulated Departure from Mean (NADM) method to assess flood dynamics, and examines the role of synoptic-scale low-pressure systems and El Niño events in modulating monsoonal rainfall and associated flood patterns.

1.1. *Kaveri River: geomorphic and climatic setting*

The Kaveri Basin is located between latitudes 10°92'–13°30' North and longitudes 75°27'–79°54' East (Fig. 1). It spans across the states of Tamil Nadu, Karnataka, Kerala and the Union Territory of Puducherry. The river rises at an elevation of 1341 m at Talakaveri, situated in the Bhramagiri Ranges of the Western Ghats in the Kodagu district of the Karnataka State. Flowing south-eastward across the Mysore Plateau it enters Tamil Nadu plains and eventually drains into the Bay of Bengal. The river spans 800 km in length and drains an area of 81,155 km². The major tributaries of the Kaveri River are the Hemavati, Kabini, Shimsha, Akravathy and Bhavani. The Kaveri Basin is bordered by the Western Ghat to the west and the Eastern Ghat to the east and south. The basin is separated by ridges to the north that divide it from the Krishna and Pennar Basins. The Kaveri Basin consists of two main geomorphic regions, the western Mysore Plateau, characterized by expansive valleys and gently sloping streams, and the eastern Tamil Nadu plains, which exhibit fluvial and deltaic features with Quaternary sediments (Kale *et al*., 2014; Mahadev, *et al*., 2025). The Kaveri Basin is largely underlain by crystalline rocks of Archaean–Proterozoic age, comprising gneisses, charnockites, and granites (Sharma & Rajamani, 2001; Valdiya, 2001). The basin is characterized by numerous lineaments, faults and shear zones, trending both north-south and east-west, which extend across the Kaveri Basin as well as the adjacent regions (Ramasamy, 2006; Vaidyanadhan, 1971; Valdiya, 2001).

The Kaveri Basin is primarily governed by the southwest monsoon in Karnataka and Kerala, and by the combined effects of the southwest and northeast monsoons in Tamil Nadu. The average annual rainfall in the basin ranges from over 2500 mm in the headwaters (Western Ghat) to approximately 700 mm in the lower

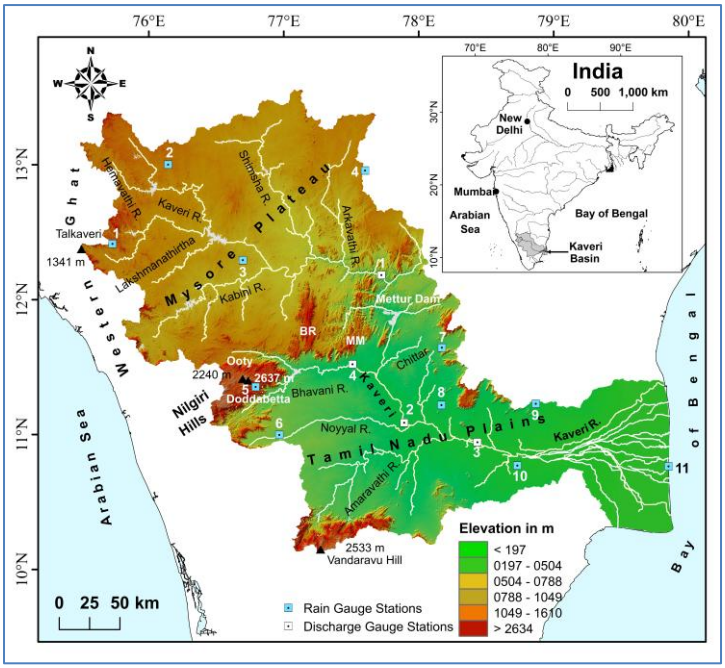

Fig. 1 Physiography of the Kaveri Basin; Locations of raingauge stations: 1 = Kodagu, 2 = Hassan, 3 = Mysore, 4 = Bangalore Urban, 5 = Connor, 6 = Coimbatore, 7 = Salem, 8 = Namakkal, 9 = Perambalur, 10 = Tiruchirappalli, 11 = Nagapattinam; Locations of discharge gauge stations (G/D): 1 = Biligundulu, 2 = Kodumudi, 3 = Musiri, 4 = Savandapur; BR = Biligirirangan Ranges, MM = Mahadeswaramalai Ranges

reaches (Kale, *et al*., 2014), with an average annual rainfall of the basin being 1172 mm (Pagare, *et al*., 2025a; Pagare, *et al*., 2025b). In excess of 75% of the basin's mean annual rainfall and corresponding surface runoff is generated during the southwest monsoon period, during which hydrodynamic conditions facilitate the mobilisation and downstream conveyance of approximately 85% of the total annual fluvial sediment load (Vaithiyanathan *et al*., 1992). The Kaveri Basin has an average annual runoff of about 21.4 km³ (Central Water Commission, 2020), which falls well below the runoff range of ~46–111 km³ observed in other major rivers of Peninsular India. This comparatively low fluvial yield results in exceptionally low specific discharges and basin-wide erosion rates (Kale *et al*., 2014).

2. Data and methodology

The annual rainfall data for eleven raingauge stations situated within and in the vicinity of the Kaveri Basin (Fig. 1) were obtained from the India Meteorological Department (IMD), Pune. The dataset spans for a period of approximately 121 years *i.e.* from 1901 to 2022. Moreover, the rainfall data for the Bengaluru raingauge station, covering the period from 1837 to 1900, were retrieved from the Divisional Archives Office, Mysuru, Karnataka. Extensive records of low-pressure system (LPS) trajectories covering the period from 1891 to 2023 were meticulously extracted by using the eAtlas software, an advanced analytical tool developed by the India Meteorological Department (IMD), Chennai. The annual maximum series (AMS) or stage data for the hydrological monitoring stations at Biligundulu and Musiri along the Kaveri River were procured from Central Water Commission (CWC, 2020). This comprehensive dataset encompasses a temporal duration of 45 years, corresponding to the periods from 1972 to 2017 for Biligundulu and from 1973 to 2018 for Musiri, respectively. The El Niño and Southern Oscillation (ENSO) index, as systematically documented by Wright (1989) for the epoch ranging from 1891 to 1983, has been thoroughly incorporated into the present analysis. The ENSO indices were systematically acquired from the Climate Prediction Centre (CPC) of the National Oceanic and Atmospheric Administration (NOAA) for the period subsequent to 1983.

The methodology employed in this study facilitated the analysis of interannual rainfall variability and associated floods, examination of storm trajectories, depth–area–duration (DAD) analysis of low-pressure systems (LPS), assessment of the relationship between

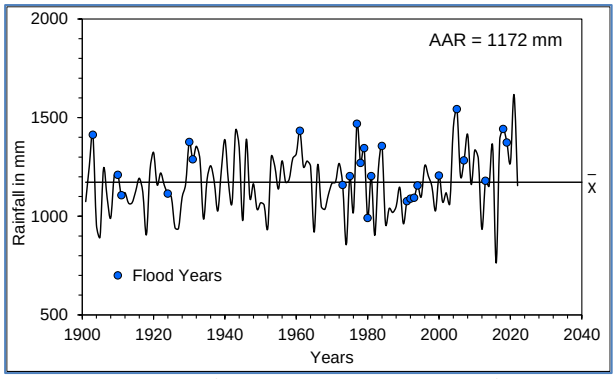

Fig. 2 Interannual rainfall variability and associated floods in the Kaveri Basin (1901 to 2022); AAR = Average annual rainfall

annual rainfall totals and flood occurrences, investigation of normalized accumulated departure from the mean (NADM), and evaluation of the influence of El Niño on monsoon rainfall. The methodological framework is rigorously articulated and critically examined in the results and discussion section.

3. Results and discussion

3.1. *Interannual rainfall variability and associated floods*

This study endeavours to elucidate the interannual variability of rainfall and its intricate association with flood occurrences within the Kaveri Basin. Analogous to other monsoon-dominated river basins in India, the Kaveri Basin displays marked interannual fluctuations in both rainfall and flood occurrence. This variability is chiefly governed by fluctuations in the intensity and frequency of rain-bearing synoptic systems, including western disturbances, cyclonic storms, monsoon depressions, and oscillations of the monsoon trough. These meteorological phenomena exert a significant influence on the spatio-temporal distribution of precipitation, thereby controlling the hydrological responses and flood dynamics within the basin.

The time series analysis of interannual rainfall variability reveals distinct phases in the rainfall pattern of the Kaveri Basin (Fig. 2). Prior to 1930, the basin experienced a predominance of below-average rainfall years, though the interannual variability during this period persisted relatively low. Between 1930 and 1985, a marked increase in above-average annual rainfall was observed, accompanied by escalated interannual variability. From 1985 to 2003, a period dominated by below-average rainfall was noted, yet interannual variability remained subdued. Since 2003, the region has experienced a resurgence of above-average rainfall years, accompanied by increased interannual variability. This contemporary period is further distinguished by a marked increase in extreme hydrological events, including amplified flood peaks and more pronounced droughts, surpassing both the frequency and intensity of comparable events in earlier phases, thereby indicating a shift towards a more erratic and extreme climatic regime.

Interannual variability in the Kaveri Basin is characterized by a notable increase in the frequency and magnitude of flood events, particularly post-1950s. A closer examination of Fig. 2 reveals that a substantial majority of the large magnitude flood events- specifically, 17 out of 26 (65%) coincided with periods of above-average rainfall, underscoring the significant role of rainfall anomalies in modifying flood dynamics within the basin.

Hire (2000) documented suppressed interannual variability with predominantly below-average rainfall in the Tapi Basin prior to 1930, transitioning to a phase of heightened variability and above-average precipitation from the 1930s to 1990s. Kale (1999) reported that this period (1930-1990) was marked by pronounced interannual variability, manifested in the elevated frequency and intensity of flood events on the Tapi River. Inter-monsoon variability within the Mahi (Pawar and Hire, 2018), Par (Patil and Hire, 2020), Damanganga (Anwat, 2022) and Upper Godavari (Patil, *et al*., 2024) Basins exhibited a pronounced intensification, characterized by a significant increase in the frequency and magnitude of flood events, predominantly commencing in the post-1930s period.

3.2. *Characteristics of the flood-generating low-pressure systems (LPS)*

India has been subject to cyclonic disturbances, including depressions and cyclonic storms, throughout the year, with the exception of February (Dhar *et al*., 1984a). According to Rao (1976), monsoon depressions are low-pressure systems (LPS) characterized by two or three closed isobars, typically spanning an area of approximately five degrees square. These LPS, primarily originates in the Bay of Bengal (around 18°N), generally propagate west-north-westward, often reaching the central regions of India. Besides, LPS, associated storm surges and resultant floods are prevalent along the south-eastern coastline of India, with notable intensity in the Puducherry, Cuddalore Districts (Duraisamy, *et al*., 2024) and the deltaic region (Hemingway, 1906; Barber, 1940; Baliga, 1957) of the Tamil Nadu state.

During the progression, LPS induce widespread and intense rainfall, particularly in the southwest quadrant, before dissipating. The associated heavy precipitation is

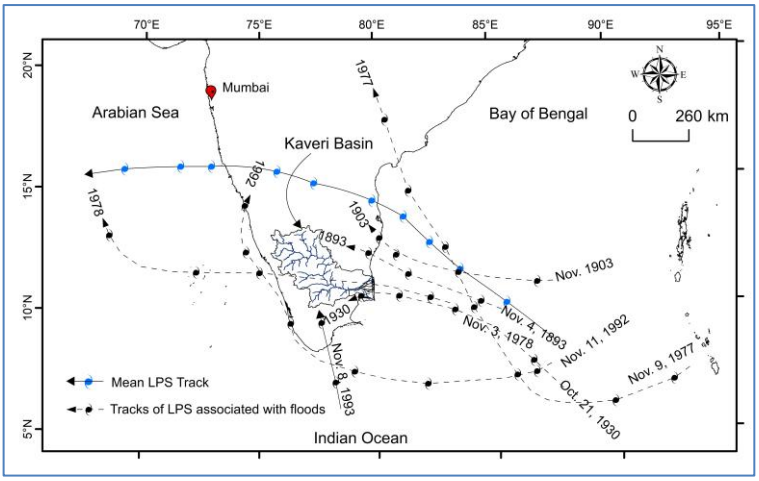

Fig. 3. Mean Low-Pressure System (LPS) trajectory with tracks of LPS responsible for major floods in the Kaveri Basin, 1891–2023

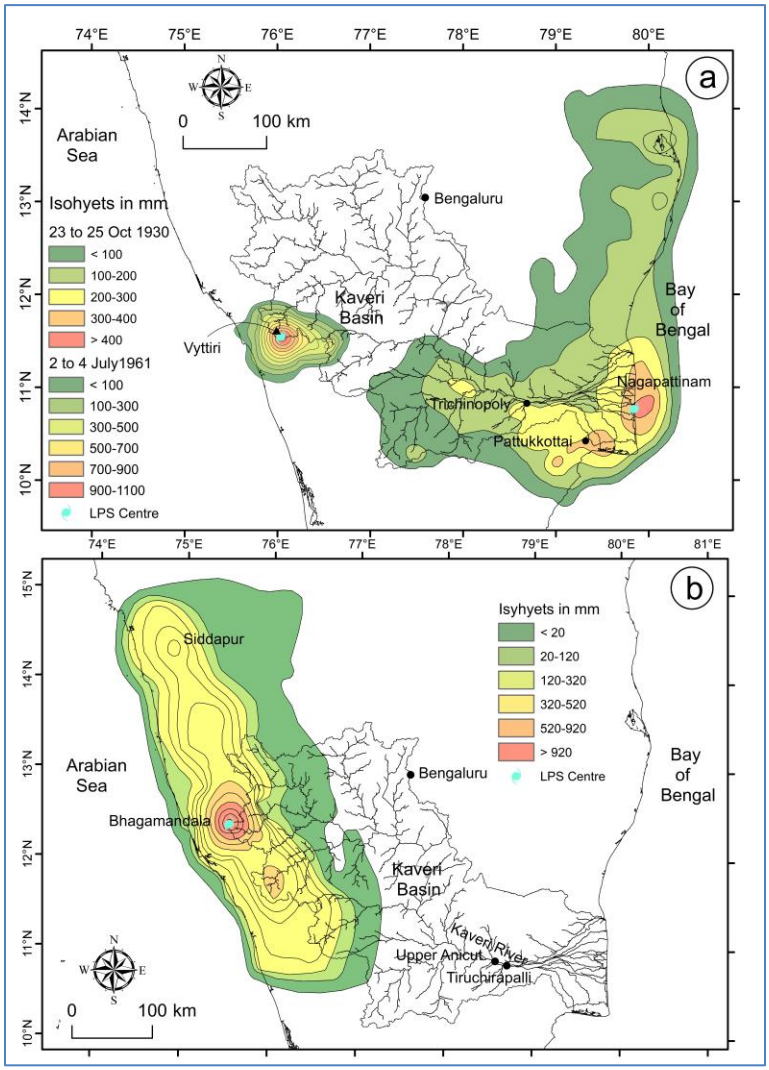

Figs. 4(a-b). a = 23-25 October 1930 and 2-4 July 1961 LPS(s) over the Kaveri Basin; b = The 3-day isohyetal (mm) pattern of 23-25 July 1924 over the Kaveri Basin; Data Source: CWC and IMD, 2015

concentrated in a narrow band approximately 400 km in width and 500 km in length, situated to the left of the disturbance's trajectory (Rao, 1976). The extreme rainfall linked to cyclonic disturbances frequently result in significant floods in river systems whose catchment areas fall within the affected rainstorm zones (Dhar, *et al*., 1984a). Such flood events are usually associated with the highest peak discharges recorded in long-term flood time series (Kale, *et al*., 1994).

Therefore, to examine the correlation between LPS and flood events in the Kaveri Basin, a systematic analysis was conducted to identify and investigate the tracks of LPS responsible for generating the highest discharge magnitudes in the region. The LPS track data were obtained using eAtlas software from IMD, Chennai and analysed using ArcGIS 10.8.1. A buffer zone of five-hundred km was delineated around the periphery of the basin and LPS tracks (Fig. 3) traversing this zone were selected for analysis (Patil and Hire, 2020). Furthermore, to determine the mean track of LPS affecting the basin, land depressions and westward-moving LPS tracks originating from the Bay of Bengal have been selected for analysis. Besides, the association between LPS and resulting floods have been assessed using the AMS/stage data and archival flood records.

The examination of synoptic conditions linked to flood-generating LPS in the Kaveri Basin indicates that while not all, a significant number of these systems originate from Bay depressions. Analysis of LPS tracks over 132 years of time span (1891-2023) reveal that 364 tracks passed through the buffer zone. The identified LPS tracks were categorized based on their origin into three distinct groups: 314 LPS developed over the Bay of Bengal, 49 LPS formed over the Arabian Sea, and a single LPS originated in the Indian Ocean, followed a south-to-north path and caused flooding in the basin.

The rainfall field remains flat in the quadrants located to the right of the depression track (Mooley, 1973). However, significant rainfall gradients are observed in the left quadrants, particularly along and west of the 80°E. The highest rainfall occurs in the left-front quadrant, roughly 150 km from the depression centre and 50–150 km away from its track (Mooley, 1973). Notably, the Kaveri Basin is positioned within the left front quadrant of the mean trajectory of LPS (Fig. 3) that travel in a west-northwest (WNW) direction, which plays a pivotal role in triggering floods in the Kaveri Basin.

Flood magnitudes associated with cyclonic events exhibit spatial variability across different reaches of the Kaveri River and its tributaries. A notable instance is the LPS of November 3, 1978, which caused significant flooding in the Kaveri Basin (Table 1). On November 5, 1978, a peak discharge of 4,079 m^3s^{-1} (>Q mean i.e. 1,485 m^3s^{-1}) was recorded at the Kodumudi G/D station (Fig. 1 and 3), located in the middle reaches of the basin.

Another LPS of October 21, 1930, caused extreme rainfall in the Kaveri Basin, with 24-hour rainfall totals of 318 mm at Trichinopoly and 297 mm at Pattukkottai (Fig. 4a) on October 23. This resulted in severe flooding, requiring the discharge capacity at the Agniar Aqueduct to be increased from 1,359 m^3s^{-1} to 1,651 m^3s^{-1} to manage the exceptional flow (Barber, 1940). The LPS of November 11, 1992 (Fig. 3), also caused flooding, with a peak discharge of 840 m^3s^{-1} (exceeding the mean discharge of 261 m^3s^{-1}) recorded on November 17, 1992, at the Savandapur G/D station (Fig. 1) on the Bhavani River, a tributary of the Kaveri. Although a few large magnitude floods are associated with the LPS over the span of 132 years in the Kaveri Basin, the frequency and discharges associated with LPS are much lower in magnitude compared to other Indian rivers such as the Godavari (Kale, *et al*., 2002; Patil, *et al*., 2024), Tapi (Kale, *et al*., 1994; Kale, *et al*., 1997; Hire, 2000; Gunjal, 2016, Narmada (Kale, *et al*., 1994; Kale, *et al*., 1997), Mahi (Pawar and Hire, 2018; Hire, 2021), Par (Patil, 2018; Patil and Hire, 2020), and Damanganga (Anwat, 2022).

3.3. *Depth-area-duration (DAD) analysis connected with LPS*

Satakopan (1949) estimated the Damodar Basin's maximum rainfall using sophisticated approaches, notably depth–area–duration (DAD) analysis and storm transposition techniques. This work remains a seminal contribution, widely regarded as a model hydromet study in river basin research. A DAD curve depicts the decline in precipitation depth with increasing storm or drainage area for a fixed duration (Parzybok *et al*., 2009). A depth-area curve represents the maximum average precipitation depth across different spatial extents within a specified time period (World Meteorological Organization, 1969; PMP Atlas, 2015). The DAD method for rainstorm analysis relates the maximum rainstorm depth to three key parameters: depth, area and duration. This approach, as outlined by Parzybok, *et al*., (2009), aims to estimate maximum precipitation over various spatial scales and durations (*e.g*. 6, 12, or 24 hours), aiding in the calculation of probable maximum precipitation (PMP).

The DAD curves were not available for the all the flood-generating LPS. However, for the significant LPS events in the Kaveri Basin, specifically those of 1924, 1930 and 1961 some information about DAD curves is available. These events were selected for rigorous analysis due to their profound hydrological and geomorphological

TABLE 1

Synoptic meteorological setup during major flood events in the Kaveri River

Event date	Annual rainfall in mm	Monsoon rainfall in mm	Pertaining to	ENSO condition	Remark
November, 1903	1413 (+20.56%)	1103 (+22.14)	LPS	La Nina	Transit in north-east with respect to basin
1910	1210 (+3.24)	1072 (+18.72)	-	-	-
1911	1106 (-5.63)	715 (-20.82)	-	El Niño	-
July 26, 1924	1114 (-4.94)	944 (+4.54)	LPS	La Nina	Storm centre over Bhagmandala
October 23, 1930	1376 (+17.43%)	978 (+8.31)	LPS	El Niño	LPS weakens over the delta region; Storm centre over Nagapattinam
August 18, 1931	1288 (+9.89)	889 (-1.55)	-	La Nina	-
July 3, 1961	1433 (+22.27)	1124 (+24.47)	LPS	-	Storm centre over Vyttiri
July 12, 1973	1158 (-1.19)	956 (+5.87)	-	Strong La Nina	-
July 16, 1975	1203 (+2.64)	894 (-0.99)	-	Strong La Nina	-
November 13, 1977	1469 (+25.34%)	1206 (+33.55)	LPS	-	Transit in north-east with respect to basin
November 5, 1978	1270 (+8.36%)	863 (-4.43)	LPS	Weak El Niño	Transit through basin
November 20, 1979	1345 (+14.76)	1169 (+29.48)	-	Weak El Niño	-
July 5-7, 1980	991 (-15.44)	826 (-8.53)	-	-	-
September 13, 1981	1203 (+2.64)	966 (+6.98)	-	-	-
August 19, 1981	1203 (+2.64)	966 (+6.98)	-	-	-
July 5, 1984	1356 (+15.69)	955 (+5.76)	-	Weak La Nina	-
July 30, 1991	1076 (-8.19)	971 (+7.53)	-	El Niño	-
November 17, 1992	1089 (-7.08%)	782 (-13.40)	LPS	Moderate La Nina	Transit in south-west with respect to basin
November 10, 1993	1093 (-6.74)	940 (+4.10)	LPS	-	Origin at Indian Ocean, Transit towards north
July 17, 1994	1155 (-1.45)	971 (+7.53)	-	Moderate El Niño	-
October 12, 2000	1206 (+2.90)	973 (+7.75)	-	Moderate La Niña	-
October 24 & 25, 2005	1543 (+31.66%)	1353 (+49.83)	-	Weak La Nina	-
August 12 & 13, 2007	1283 (+9.47)	1050 (+16.30)	-	Strong La Nina	-
August 5 & 6, 2013	1179 (+0.59)	1048 (+16.10)	-	-	-
August 16-19, 2018	1442 (+25.60)	1161 (+28.57)	-	Weak El Niño	-
August 11, 2019	1374 (+17.24)	1146 (+26.91)	-	-	

LPS = Low-pressure systems; Numbers in brackets indicate % deviation from mean rainfall; Refer Fig. 3 and Fig. 4 a and b; Data source: e-Atlas, CWC & IMD (2015), Golden Gate Weather Services (2016); Note: Flood years are selected on the basis of information from archives, LPS, Mean +1σ flood (Large flood) at Musiri and Biligundulu sites

implications and data availability from the PMP Atlas (2015). The July 23-25, 1924 LPS (Fig. 4b) has been selected for analysis due to its exceptional meteorological significance. This system produced a remarkable 24-hour rainfall total of 842 mm on July 23, 1924 and an unprecedented 3-day peak rainfall of 1817 mm at Bhagamandala, Karnataka (Fig. 5a). The November 23-25, 1930 LPS (Fig. 4b) has been included for its hydrological impact, which induced severe flooding in the lower reaches of the Kaveri Basin (Hemingway, 1906; Barber, 1940; Baliga, 1957). The LPS of July 2-4, 1961 (Fig. 4a) has been chosen, as severe floods have been recorded during the period of 26 June to 27 July 1961 in the Kaveri Basin. Parthasarathy and Sarkar (1966) also provided a brief overview of the large-scale synoptic conditions associated with these floods.

Preparing isohyetal maps for selected LPS events is an essential first step in DAD analysis. Isohyetal patterns for the 1924, 1930, and 1961 LPS events, sourced from

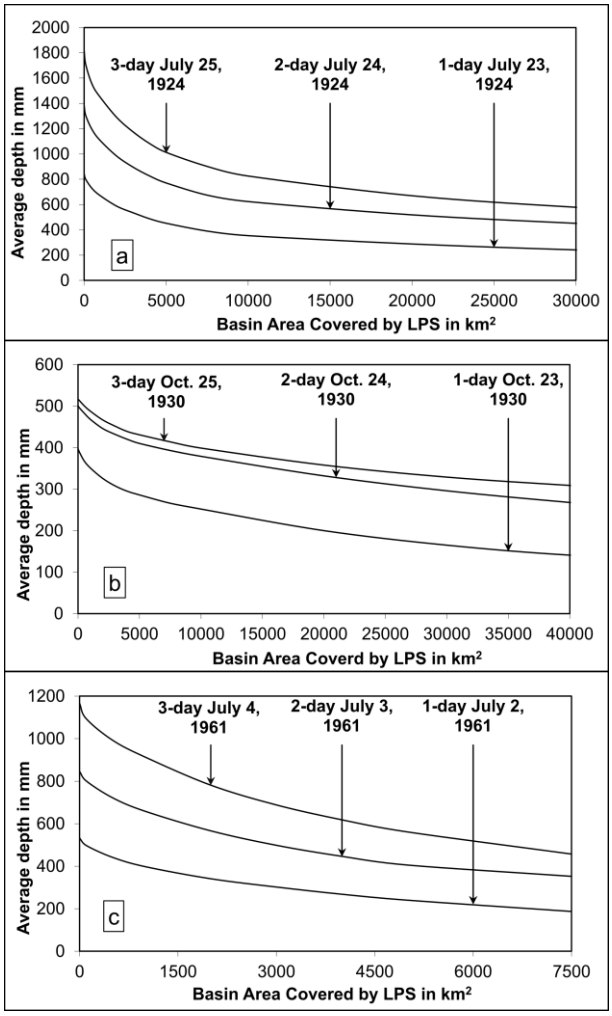

Figs. 5(a-c). DAD curves for significant LPS events in the Kaveri Basin; a = 23-25 July 1924, b = 23-25 October 1930 and c = 2-4 July 1961 event; Data source: CWC and IMD, 2015

India's isopluvial maps (Indian Institute of Tropical Meteorology, Pune) and the PMP atlas (CWC & IMD, 2015) compiled by Water and Power Consultancy Services (WAPCOS, 1998), were digitized and georeferenced in ArcGIS 10.8.1 for subsequent analysis. Additionally, average rainfall depths for 1924, 1930, and 1961, derived from the PMP Atlas (CWC & IMD, 2015), were plotted against accumulated area, and smoothed DAD curves were generated for each LPS and duration. These curves were prepared for durations of one, two, and three days for the selected LPS events.

The DAD analysis of the July 23–25, 1924 LPS (Fig. 4b) shows that this event produced the highest average rainfall depths over the Kaveri Basin for 1-day, 2-day and 3-day (842, 1,382 and 1,817 mm respectively) (Fig. 5a) duration. This event has caused 13,000 m^3s^{-1} at Tiruchirappalli and highest ever recorded flood levels and discharges (Q) at upper anicut and ~1.6 km upstream of grand anicut (Q = 13,097 and 13,450 m^3s^{-1} respectively) (Barber, 1940)).

The centre of the 1930 LPS for 1-day, 2-day and 3-day duration was located at Nagapattinam (Fig. 4a) (10°46.012'N° N 79°50.629'E) in the Tamil Nadu state (CWC and IMD, 2015). The DAD curve of 23-25 October 1930 event has imparted 398, 501- and 517-mm average depth of rainfall over the basin for 1-day, 2-day and 3-day duration respectively (Fig. 5b). The centre of LPS for July 1961 was located at Vyttiri (11°33.100'N & 76°2.416'E) (Fig. 4a; Table 1) in Kerala State for 1-day, 2-day and 3-day duration. The DAD curve for the event of July 4-6, 1961, produced an average depth of rainfall over the basin for 1-day, 2-day, and 3-day durations, with measurements of 533 mm, 846 mm, and 1166 mm, respectively (Fig. 5c). The maximum observed flood peak recorded after the passage of LPS was 7,789 m^3s^{-1}, i.e. on 8th July 1961 at Mettur Dam. This significant hydrological event led the CWC to approve a revised design flood of 18,681 m^3s^{-1}, which is approximately 48% higher than the original design flood of 12,547 m^3s^{-1} (Water Resources Department, Government of Tamil Nadu, 2021).

The DAD curves delineated for the Tapi, Par and Mahi Bains (Hire, 2000; Patil and Hire, 2020; Pawar, 2019) elucidate that the rainfall depths and resultant flood generation patterns in the Kaveri Basin differ markedly from the aforementioned basins. For instance, the largest average depth of rainfall during the 1968 LPS event over the Tapi Basin up to Ukai (A = 62,224 km²; Q = 42,450 m^3s^{-1}) for a 3-day storm was 249 mm (Hire, 2000). The DAD curve for the 4-6 August 1968 event resulted in substantial average rainfall depths of 437 mm (1-day), 705 mm (2-day), and 932 mm (3-day) across the Par Basin. Consequently, this flood culminated in the highest gauged flood levels (A = 1,252 km²; Q = 23,820 m^3s^{-1}) on the Par River at Nanivahial (Patil, 2018; Patil and Hire, 2020). Moreover, the DAD curve for the 26-28 July 1927 storm contributed the highest average rainfall depth of 650 mm over three days in the lower Mahi Basin, Gujarat. Nonetheless, the event did not engender the highest flood levels, as the rainstorm centre was at Dakor, adjacent to the basin, with the storm confined to the lower reaches of the basin. A cursory comparison highlights that, although, Kaveri Basin, was subjected to considerable rainfall depths, it did not exhibit the extreme flood magnitudes characteristics like the Tapi, Par, and Mahi Basins.

3.4. *Relationship between annual rainfall totals and flood occurrences*

Fig. 6 (a-b) presents the departures of average annual rainfall in the Kaveri Basin and the discharge at the

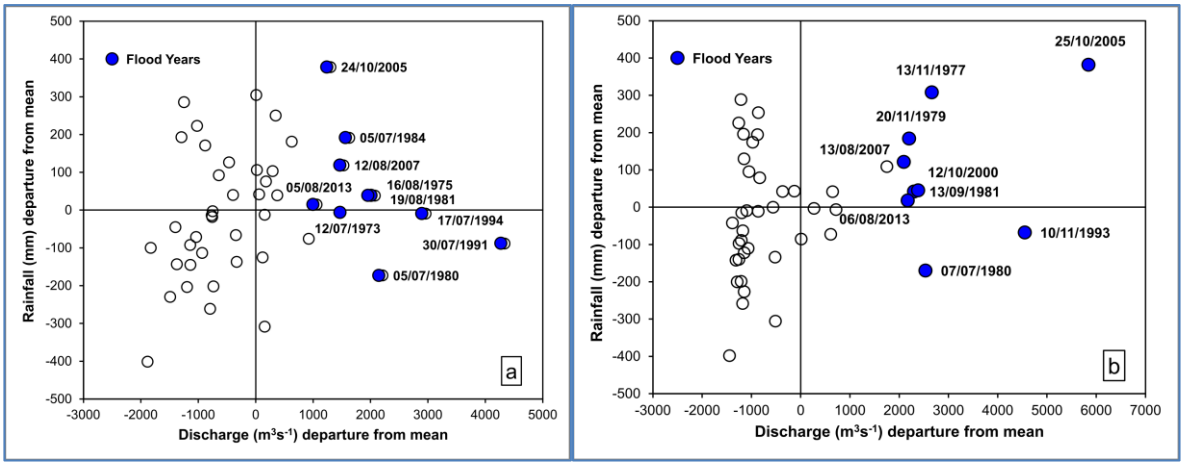

Figs. 6(a-b). a = Discharge (Q) (Biligundulu G/D site) and Rainfall (Average annual rainfall of the basin) departure from mean; b = Discharge (Q) (Musiri G/D site) and Rainfall (Average annual rainfall of the basin) departure from mean

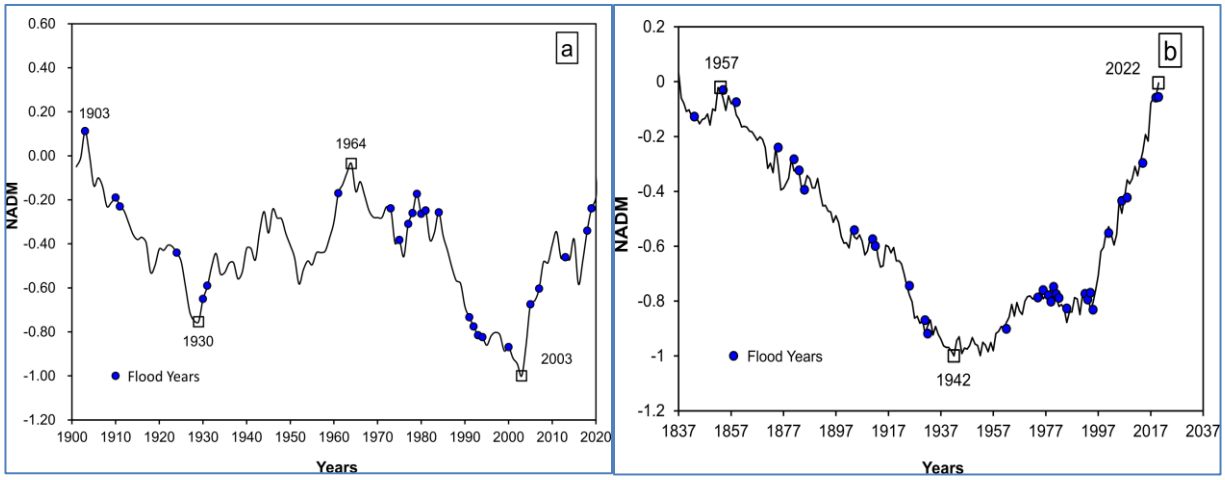

Figs. 7(a-b). a = Normalized Accumulated Departure from Mean (NADM) (Kaveri Basin); b = NADM (Bengaluru)

Biligundulu and Musiri discharge gauging (G/D) stations (Fig. 1) from their respective long-term averages. The graphs highlight that major floods at Biligundulu (1975, 1981, 1984, 2005, 2013) and Musiri (1977, 1979, 1981, 2000, 2005, 2007) sites have primarily occurred during years of above-average annual rainfall. Interestingly, the floods observed in 1973, 1980, 1991 and 1994 at the Biligundulu site, as well as those in 1980, 1993 and 2013 at the Musiri site, represent hydrological anomalies, as they occurred during years of below-average annual rainfall. Notably, 2005 is distinguished as the year with the highest average annual rainfall in the Kaveri Basin (1,543 mm), leading to the highest recorded discharge at the Musiri site (7,690 m^3s^{-1}). This phenomenon may be ascribed to the occurrence of intense flood-generating precipitation events. The Tapi River (Hire, 2000), the Par River (Patil and Hire, 2020), the Mahi River (Pawar, 2019) exhibit similar depictions. However, the 1968 flood, the largest of the 20th century on the Tapi (Hire, 2000) and the Par River (Patil and Hire, 2020), but only a mediocre flood on the Mahi River (Pawar, 2019), occurred in a below-average rainfall year.

3.5. *Normalized accumulated departure from mean (NADM) and floods*

Monsoonal rainfall in a region exhibits significant interannual variability, with deviations from the long-term mean showing marked inconsistency and variation between different years (Gadgil, 2002). The Normalized Accumulated Departure from Mean (NADM) statistical method provides an effective approach for analysing successive attributes in long-term datasets (Riehl, *et al*., 1979; Mooley and Parthasarathy, 1984; Probst and Tardy, 1987; Kale, 1999). This statistical technique is commonly employed in research on rainfall variability (Kale, 1999; Hire, 2000; Gunjal, 2016; Patil, 2018; Pawar and Hire, 2018; Patil and Hire, 2020). The NADM method reduces short-term fluctuations, highlighting long-term variability in streamflow and monsoonal rainfall patterns.

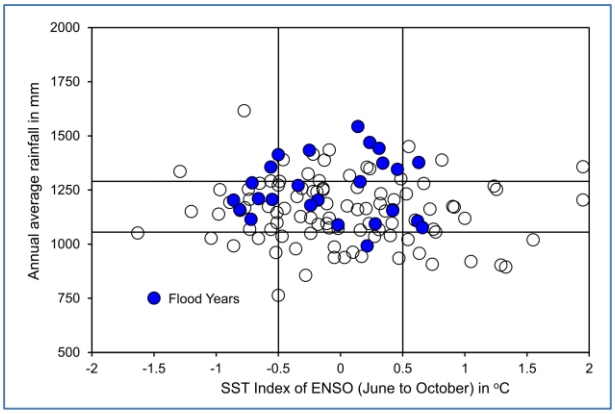

Fig. 8. Annual rainfall and ENSO index categories for the Kaveri Basin; sources: India Meteorological Department (IMD); National Oceanic and Atmospheric Administration (NOAA)

NADM is calculated by scaling the accumulated departure from mean (ADM) through division by its maximum absolute value, restricting the range to -1 and +1 (Thomas, 1993). This method facilitates both apparent and statistical correlation of heterogeneous datasets (Thomas, 1993). Periods exhibiting above-average conditions are generally represented by positive gradients in graphical analyses, whereas below-average conditions are denoted by negative gradients (Gregory, 1989; Thomas, 1993). Unlike other methods, such as running means, the ADM clearly emphasizes the differences between periods of high and low rainfall (Probst and Tardy, 1987). To calculate the NADM for the Kaveri Basin, annual average rainfall data (1901-2022 for the Kaveri Basin and 1837-2020 for the Bangalore raingauge station located on the border of the basin (Fig. 1)) and Annual Maximum Series (AMS) data for Musiri G/D site (1973-2017) were utilized to represent the flood events (Fig. 7, a-b).

The NADM graph presented in Fig. 7 a-b delineates the long-term rainfall trends for the Kaveri Basin and Bengaluru raingauge station and provide a comprehensive analysis of its temporal variability.

The ascending (descending) slope of the NADM graph signifies periods of above-average (below-average) rainfall conditions.

The NADM analysis reveals a period of below-average rainfall during the early 20th century, extending to 1930 (Fig. 7a). The subsequent interval, from 1930 to 1964, is characterized by a pronounced positive anomaly in the NADM curve, indicative of sustained above-average rainfall conditions. The period from 1964 to 2003 is characterised by below-average rainfall conditions and the time span 2003 to 2022 show above-average rainfall conditions. Deriving a definitive conclusion about the rainfall patterns in the Kaveri Basin from the above illustrations is challenging, however, the pattern highlights certain overarching characteristics of the rainfall behaviour of the basin.

(*i*) 1901–1930 is characterized by below-average (low) rainfall regime.

(*ii*) The interval 1930–1964 corresponds to a phase of above-average (high) rainfall.

(*iii*) 1964 to 2003 is associated with below-average rainfall conditions.

(*iv*) Above-average (high) rainfall period is observed from 2003 to 2022.

The analysis of the annual rainfall data for the Kaveri Basin, focusing on deviations in rainfall amounts, distinctly highlights significant shifts occurring around 1930, 1964 and 2003. Prior to 1960, comparable major transitions in monsoon conditions have been identified by Mooley and Parthasarathy (1984), Fu and Fletcher (1988), Parthasarathy *et al.* (1991), Kripalani and Kulkarni (1997), Pawar and Hire (2018) and Patil and Hire (2020) for similar periods in India. The association of all-India monsoon rainfall (Parthasarathy, *et al.*, 1991) with the rainfall of the Kaveri Basin shows remarkable similarity in their long-term fluctuations till 1960.

The NADM graph presented in Fig. 7b demonstrates the long-term temporal trends of rainfall patterns spanning 183 years. The graph distinctly delineates a protracted period of below-average (low) rainfall from 1857 to 1942, followed by a sustained phase of above-average (high) rainfall from 1942 to 2020 with slight fluctuations in the latter period. While continuous flood magnitude data prior to 1970 is sparse, the extant records enable reasonable inference of non-random long-term flood responses. This suggests a discernible pattern wherein periods of above-average (high) and below-average (low) monsoon rainfall and discharge conditions exhibit a tendency to cluster.

3.6. *El Niño and Southern Oscillation (ENSO) and floods*

The El Niño–Southern Oscillation (ENSO) is a large-scale coupled ocean-atmosphere circulation phenomenon in the equatorial Pacific (Chiew and McMahan, 2002). It is recognized as a dominant driver of rainfall anomalies, impacting the occurrence of floods and droughts in numerous regions worldwide, including India (Ropelewski and Halpert, 1987; Kane, 1989; Simpson, *et al.*, 1993; Lutgens and Tarbuck, 1995). Fluctuations in monsoonal rainfall and associated flood events exhibit a

TABLE 2

Probabilistic relationship between Kaveri Basin monsoon rainfall and the ENSO SST index (N = 121 years)

Region	AAR	SST		
		Cold	Average	Warm
Kaveri Basin	High	0.16	0.25	0.16
	Normal	0.66	0.55	0.56
	Low	0.19	0.20	0.28

Data source: IMD and Wright (1989); Low <10% AAR and High >10% AAR; AAR = Average Annual Rainfall

TABLE 3

Flood occurrence and its relationship with annual rainfall and the ENSO SST index

Region	AAR	SST		
		Cold	Average	Warm
Kaveri Basin	Above Normal	1903, 1984	1961,1977, 1979, 2005, 2018, 2019	1930
	Normal	1910, 1924, 1973, 1975, 2000, 2007	1931, 1978, 1981, 1992, 1993, 1994, 2013	1911, 1991
	Below Normal	1980		

Data source: IMD and Wright (1989); Low <10% AAR and High >10% AAR; AAR = Average Annual Rainfall.

significant correlation with ENSO variability (Bhalme and Jadhav, 1984; Burn and Arnell, 1993). El Niño, the warm phase of ENSO, is linked to weakened Indian monsoon rainfall and a truncated rainy season, while La Niña, the cold phase, correlates with elevated rainfall and extended monsoon duration (Kripalani *et al*., 2003; Panda and Kumar, 2014; Panda *et al*., 2014; Dwivedi *et al*., 2015). Kale, *et al*., (1996) reported that several modern and historical flood events were found to coincide with the ENSO events.

The rainfall, and by extension flood incidence, within the basin is acutely sensitive to perturbations in the Indian southwest monsoon, which maintains teleconnections with ENSO phenomena. Consequently, an investigation has been undertaken to delineate the intrinsic variability of annual rainfall and concomitant flood events in the Kaveri Basin and to evaluate their correspondence with ENSO episodes.

The ENSO phenomenon is characterized by a monthly time series of mean sea surface temperature (SST) anomalies computed over the central and eastern Pacific Ocean. The index used in this study is further averaged over the monsoon season (June-October). The analytical method employed follows the approach outlined by Eltahir (1996) for the Nile River. In accordance with Eltahir (1996), SST values were categorized into cold, warm, and normal phases using temperature thresholds of -0.5 °C and +0.5 °C. The conditional probabilities of rainfall were then calculated to assess the relationship between rainfall magnitude and ENSO conditions in different years, with the results presented in Table 2.

The analysis indicates a 16% probability of anomalously high monsoon rainfall and consequent flooding in the Kaveri Basin under La Niña (cold ENSO) conditions, compared to a 28% probability of deficient rainfall during El Niño (warm ENSO) phases (Fig. 8 and Table 2). Moreover, the outcomes of the conditional probability assessment, together with flood incidence data, reveal a definitive linkage between annual mean rainfall and the ENSO SST index during the June-October monsoon season. Flood years, marked by blue circles, typically occur with moderate to high rainfall (1000-1500 mm) and are associated with a neutral to weak El Niño phase (SST index between -1.0 and 0.5°C). This, therefore, suggests that floods are more likely in years with neutral or weak ENSO conditions.

Kripalani *et al*. (2003) observed that the warm ENSO phase (El Niño) is typically associated with a reduction in Indian monsoon rainfall, whereas the cold phase (La Niña) corresponds to enhanced monsoon precipitation. This analysis aligns with the conditional probability and occurrence of floods in the Kaveri Basin. It is noteworthy that the majority of floods in the Kaveri Basin have occurred under conditions of normal to above-normal rainfall and average temperatures.

The notable 1924 flood in the Kaveri Basin (Barber, 1940; Mahadev, *et al*., 2025), which is associated with a negative SST index value (approximately -1.0 to 0°C), indicates that the flood occurred during year of moderate to high rainfall, corresponding to a cold normal phase or La Niña conditions in the ENSO cycle (Table 3).

Kale, *et al*. (1996) concluded that numerous modern and historical flood events were found to coincide with the ENSO events. Pawar and Hire (2018) confirmed that the probability of high monsoon rainfall in the Mahi Basin is greater under cold and normal ENSO conditions (32%–39%) and considerably lower during warm ENSO phases (54%). Patil and Hire (2020) reported that flood frequency is generally elevated during average ENSO SST indices, with the majority of floods in the Par Basin occurring under above-normal rainfall conditions.

4. Conclusions

Time series analysis of annual mean rainfall over the Kaveri Basin reveals marked interannual variability, closely aligned with fluctuations in flood frequency and magnitude. Long-term temporal trends in the annual average rainfall of the basin reveal distinct anomalies, with specific years characterized by significantly above-average (high) or below-average (low) monsoon rainfall,

directly modulating flood intensities and hydro-meteorological dynamics. Interannual variability in the Kaveri Basin is characterized by a notable increase in the frequency and magnitude of flood events, particularly post-1930s. Moreover, substantial flood events coincided with periods of above-average rainfall, underscoring the significant role of rainfall anomalies in controlling flood dynamics within the basin. The Kaveri Basin occupies the southern fringe of the Bay of Bengal synoptic depression corridor, rendering it particularly susceptible to intense rainfall episodes induced by low-pressure systems (LPS), especially in the deltaic zone. Correlative analysis of mean annual rainfall in the Kaveri Basin and discharge deviations at the Musiri site on the Kaveri River demonstrates that major flood events, notably in 2005, coincided with years of above-average rainfall. This year recorded the second-highest average annual rainfall (1543 mm) in the basin. Periodization of monsoonal rainfall variability demarcates four distinct epochs: 1901–1930 (deficient rainfall), 1930–1964 (enhanced rainfall), 1964–2003 (reduced rainfall), and 2003–2022 (high rainfall resurgence). NADM-based diagnostics further corroborate this linkage, showing flood occurrences primarily along the rising limb (above-average rainfall periods), with fewer yet non-negligible events on the falling limb (dry anomalies). Moreover, conditional probability analysis indicates that flood frequency in the Kaveri Basin is generally elevated during years characterized by neutral or weak ENSO conditions, underscoring the limited deterministic influence of strong ENSO phases on regional flood dynamics.

Acknowledgments

This research is supported by Anusandhan National Research Foundation (Former Science and Engineering Research Board), Department of Science and Technology, Government of India (Project File No. CRG/2022/000823 dated September 1, 2023) to Pramodkumar Hire and Archana Patil. This study is also supported by the ICSSR Centrally-Administered Full-Term Doctoral Fellowship for 2024–25 (ICSSR/RFD/24-25/GEOG/GEN/144, dated February 6, 2025), awarded to Smita Pagare. The authors are obligated to India Meteorological Department, Pune and Chennai and Central Water Commission, New Delhi for providing meteorological and hydrological data respectively. The authors acknowledge the Divisional Archives Office, Mysore, for providing historical data on the floods of the Kaveri River and the Karnataka Engineering Research Station (KERS), Mandya District, for granting access to their library resources. The authors are thankful to Professor Vishwas S. Kale for his helpful and constructive comments and suggestions. Authors are grateful to Gitanjali Bramhankar and Abhinav Khare for assistance in the field. The authors also gratefully acknowledge the support extended by the research centre at HPT Arts and RYK Science College, Nashik – 422005, India, affiliated with Savitribai Phule Pune University, for providing the academic infrastructure and resources vital to the successful completion of this research.

Funding

This research is supported by the Anusandhan National Research Foundation (formerly Science and Engineering Research Board), Department of Science and Technology, Government of India (Project No. CRG/2022/000823, dated September 1, 2023) awarded to Pramodkumar Hire and Archana Patil. Additional support was provided by the ICSSR Centrally-Administered Full-Term Doctoral Fellowship for 2024–25 (ICSSR/RFD/24-25/GEOG/GEN/144, dated February 6, 2025), awarded to Smita Pagare.

Data availability

Data available on request due to privacy/ethical restrictions.

Authors' Contribution

Pramod kumar Hire: Oversight of manuscript review and editing, supervision, methodological design, execution of investigations, and acquisition of research funding. (*email: pramodkumarhire@gmail.com*)
Smita Pagare: Formal analyses, comprehensive data curation, and Funding acquisition. (*email:* smitapagare *2020@gmail.com*)
Archana Patil: Original manuscript drafting, formal data analyses, conceptualization, and attainment of research funding.

Disclaimer: The authors declare the following financial interests/personal relationships which may be considered as potential competing interests:

References

Anwat, V.K., 2022, "Fluvial and flood geomorphological investigations of bedrock channel reaches of the Damanganga River", Ph.D. Dissertation, Savitribai Phule Pune University, Pune, India.

Baliga, B.S., 1957, "Tanjore District Handbook", *Government Press*, Madras.

Banerji, S. and Narayanan, J., 1966, "The importance of Cauvery watershed in causing floods in the Madras plains", *Indian Journal of Meteorology & Geophysics*, **17**, 23–30.

Barber, W.H., 1940, "History of the Cauvery Mettur Project", *Government Press*, Madras.

Bhalme, H.N. and Jadhav, S.K., 1984, "Southern Oscillation and its relation to the monsoon rainfall", *Journal of Climatology*, **4**, 5. 509–520, doi: https://doi.org/10.1002/joc.3370040506.

Burn, D.H. and Arnell, N.W., 1993, "Synchronicity in global flood responses", *Journal of Hydrology*, **144**, 1-4. 381-404, https://doi.org/10.1016/0022-1694(93)90181-7.

Central Water Commission (CWC) and India Meteorological Department (IMD), 2015, *PMP Atlas for Cauvery and Other East Flowing River Basins: Final Report*, Volume I, Prepared by RMSI, Noida, India. Available at: https://indiawris.gov.in/wris/

Central Water Commission (CWC), 2020. Water Year Book 2018–19, *Cauvery Basin, Cauvery & Southern Rivers Circle*. *Stream Flow & Suspended Sediment Data*, Volume I. Bengaluru, India. Available at: Central Water Commission – Water Year Book 2018–19.

Chiew, F.H.S. and McMahon, T.A., 2002, "Global ENSO–streamflow teleconnection, streamflow forecasting, and interannual variability", *Hydrological Sciences Journal*, **47**, 3. 505–522, doi: https://doi.org/10.1080/02626660209492950.

Dhar, O.N., Kulkarni, A.K. and Mandal, B.N., 1984a, "The most severe rainstorm of India - a brief appraisal", *Hydrological Sciences Journal*, **29**, 2. 219–229, doi: https://doi.org/10.1080/02626668409490932.

Duraisamy Rajasekaran, S.K., Radhakrishan, S., Veeramalai, G., Huang, X. and Ayyamperumal, R., 2024, "Quantifying regional rainfall dynamics in southern India: Unravelling monsoon characteristics and intense precipitation using satellite and observed data records", *Physics and Chemistry of the Earth, Parts A/B/C*, **135.** 103642, doi: https://doi.org/10.1016/j.pce.2024.103642.

Dwivedi, S., Goswami, B.N. and Kucharski, F., 2015, "Unravelling the missing link of ENSO control over the Indian monsoon rainfall", *Geophysical Research Letters*, **42**. 8201–8207, doi: https://doi.org/10.1002/2015GL065137.

Eltahir, E.A.B., 1996, "El Niño and the natural variability in the flow of the Nile River", *Water Resources Research*, **32**. 131–137, doi: https://doi.org/10.1029/95WR03217.

Fu, C. and Fletcher, J., 1988, "Large signals of climatic variations over the ocean in the Asian monsoon region", *Advances in Atmospheric Sciences*, **5**. 389–404, doi: https://doi.org/10.1007/s00376-988-0037-0.

Gadgil, A., 2002, Rainfall characteristics of Maharashtra. In Diddee, J., Jog, S.R., Kale, V.S. and Datye, V.S. (Eds.), *Geography of Maharashtra*, 89–102. Rawat Publications, Jaipur.

Golden Gate Weather Services, 2016, "*El Niño and La Niña years and intensities"*. Available at: http://ggweather.com/enso/oni.htm.

Gregory, S., 1989, "Macro-regional definition and characteristics of Indian summer monsoon rainfall 1871-1985", *International Journal of Climatology*, **9**. 465–483, doi: https://doi.org/10.1002/joc.3370090504.

Gunjal, R.P., 2016, "Rainfall characteristics of the Tapi basin", Ph.D. Dissertation, Tilak Maharashtra Vidyapeeth, Pune, India.

Hemingway, F.R., 1906, "Madras District Gazetteers: Tanjore", Francis W. (Ed.). *Government Press*, Madras.

Hire, P.S., 2000, "Geomorphic and hydrologic studies of floods in the Tapi Basin", Ph.D. Dissertation, University of Pune, Pune, India.

Hire, P.S., 2021, "Evaluation of the flood hydrology and geomorphology in the Upper Mahi Basin using palaeoflood, historical, and modern records". Funded by Anusandhan National Research Foundation (ANRF), Government of India, New Delhi.

Hirschboeck, K.K., 1988, "Flood hydroclimatology", In: Baker, V.R., Kochel, R.C., Patton, P.C. (eds), *Flood Geomorphology*, Wiley. 27–49.

Kale, V.S., 1999, "Long-period fluctuations in monsoon floods in the Deccan Peninsula, India", *Journal of Geological Society of India*, **53,** 1. 5-15.

Kale, V.S., Deodhar, L.A. and Hire, P.S., 2002, "Rivers of Maharashtra: Their hydrology and sediment pattern", In: Diddee, J., Jog, S.R., Kale, V.S., Datye, V.S. (eds), *Geography of Maharashtra*, Rawat Publications, Jaipur. 72-80.

Kale, V.S., Ely, L.L., Enzel, Y. and Baker, V.R., 1994, "Geomorphic and hydrologic aspects of monsoon floods on the Narmada and Tapi Rivers in central India", *Geomorphology*, **10**, 2. 157–168, doi: https://doi.org/10.1016/0169-555X(94)90018-6.

Kale, V.S., Ely, L.L., Enzel, Y. and Baker, V.R., 1996, "Palaeo and historical flood hydrology", Indian Peninsula, In: Branson, J., Brown, A.G., Gregory, K.J., (eds), *Global Continental Changes: The Context of Palaeohydrology*, Geological Society Special Publication, **115**. 155–163.

Kale, V.S., Hire, P.S. and Baker, V.R., 1997, "Flood hydrology and geomorphology of the monsoon-dominated rivers: The Indian Peninsula", *Water International*, **21**. 259-265.

Kale, V.S., Sengupta, S., Achyuthan, H and Jaiswal, M., 2014, "Tectonic controls upon Kaveri River drainage, cratonic Peninsular India: Inferences from longitudinal profiles, morphotectonic indices, hanging valleys, and fluvial records", *Geomorphology*, **227**. 153–165, doi: https://doi.org/10.1016/j.geomorph.2013.07.027.

Kane, R.P., 1989, "Relationship between southern oscillation/El Niño and rainfall in some tropical and midlatitude regions", *Proceedings of Indian Academy of Sciences*, **98**, 223–235.

Kripalani, R.H. and Kulkarni, A., 1997, "Climatic impact of El Niño/La Niña on the Indian monsoon: A new perspective", *Weather*, **52**, 2. 39–46.

Kripalani, R.H., Kulkarni, A., Sabade, S.S. and Khandekar, M.L., 2003, "Indian monsoon variability in a global warming scenario", *Natural Hazards*, **29**, 2. 189–206. doi: https://doi.org/10.1023/A:1023695326825.

Lutgens, F.K. and Tarbuck, E.J., 1995, "The atmosphere", Prentice Hall, New Jersey.

Mahadev, Behera, D., Kumar, P., Jaiswal, M.K. and Singh, A.K., 2025, "A terrestrial record of ~3000 years of extreme floods from the Kaveri and adjacent river basins, Tamil Nadu, India". *Quaternary International*, **738**. 109856, doi: https://doi.org/10.1016/j.quaint.2025.109856.

Mooley, D.A., 1973, "Some aspects of Indian monsoon depressions and the associated rainfall", *Monthly Weather Review*, **101**, 3. 271–280.

Mooley, D.A. and Parthasarathy, B., 1984, "Fluctuation of all-India summer monsoon rainfall during 1871–1978", *Climatic Change*, 6, 3. 287–301.

Nanditha, J.S. and Mishra, V., 2024, Drivers of widespread floods in Indian river basins. *Journal of Hydrometeorology*, **25**, 11. 1593–1606. doi: https://doi.org/10.1175/JHM-D-23-0206.1.

Pagare, S.R., Hire, P.S. and Patil, A.D., 2025a, "Magnitude and Frequency Analyses of Floods on the Kaveri River of the Southern India by Using Gumbel Extreme Value Type-I Probability Distribution", *Hydrospatial Analysis*, **9**, 1. 1-9, doi: https://doi.org/10.21523/gcj3.2025090101.

Pagare, S.R., Hire, P.S. and Patil, A.D., 2025b, "Fluvial and flood regime characteristics of the Kaveri River: Southern India". *Meteorology Hydrology and Water Management. Research and Operational Applications*, **13**. 1–12, doi: https://doi.org/10.26491/mhwm/210192.

Panda, D.K. and Kumar, A., 2014, "The changing characteristics of monsoon rainfall in India during the global warming era (1971–2005) and links with large-scale circulation", *International Journal of Climatology*, **34**, 7. 2409–2420, doi: https://doi.org/10.1002/joc.3948.

Panda, D.K., Mishra, A., Kumar, A., Mandal, K.G., Thakur, A.K. and Srivastava, R.C., 2014, "Spatio-temporal patterns in the mean and extreme temperature indices of India, 1971–2005", *International Journal of Climatology*, **34**, 11. 3585–3603, doi: https://doi.org/10.1002/joc.3984.

Parthasarathy, B., Rupa Kumar, K. and Munot, A.A., 1991, "Evidence of secular variations in Indian monsoon rainfall-circulation relationship", *Journal of Climatology*, **4**, 11. 927–938.

Parthasarathy, S. and Sarkar, A.K., 1966, "A study of the 1961 flood in the Cauvery catchment", *Indian Journal of Meteorology and Geophysics*, **17**, 4. 329–336.

Parzybok, T.W., Hultstrand, D.M., Tomlinson, E.M. and Kappel, B., 2009, "Real-time depth-area-duration analysis for EAPS and flood warning systems", *Applied Weather Associates, LLC.*

Patil, A.D., 2018, "Bedrock channel of the Par River; its forms and processes", Dissertation, Tilak Maharashtra Vidyapeeth, Pune.

Patil, A.D. and Hire, P.S., 2020, "Flood hydrometeorological situations associated with monsoon floods on the Par River in Western India", *MAUSAM*, **71**, 4. 687–698, doi: https://doi.org/10.54302/mausam.v71i4.58.

Patil, A.D., Hire, P.S., Bramhankar, G.W., Gunjal, R.P., Anwat, V.K. and Khandare, P.R., 2024, "Flood Meteorology, Hydrology, and Geomorphology of the Upper Godavari River, Western India", *Meteorology, Hydrology and Water Management*, **12**, 1. 65-82, doi: https://doi.org/10.26491/mhwm/191702.

Pawar, U.V., 2019, "An Analytical Study of Geomorphological, Hydrological and Meteorological Characteristics of Floods in The Mahi River Basin: Western India", Dissertation, Tilak Maharashtra Vidyapeeth, Pune.

Pawar, U.V. and Hire, P.S., 2018, "Long term fluctuations and global teleconnections in the monsoonal rainfall and associated floods of the Mahi Basin: Western India", *International Conference on Frontiers in Life and Earth Science*, **5**, 1. 237-241.

Probst, J.L. and Tardy, Y., 1987, "Long range streamflow and world continental runoff fluctuations since the beginning of this century", *Journal of Hydrology*, **94** (3–4). 289–311, doi: https://doi.org/10.1016/0022-1694(87)90057-6.

Ramasamy, S.M., 2006, "Remote sensing and active tectonics of South India", *International Journal of Remote Sensing*, **27**, 20. 4397-4431, doi: https://doi.org/10.1080/01431160500502603.

Rao, Y.P., 1976, "Southwest Monsoon", Meteorological Monograph, Synoptic Meteorology, India Meteorological Department, Delhi, India, **1**. 07-185.

Riehl, H., El-Bakry, M. and Meitin, J., 1979, "Nile river discharge", *Monthly Weather Review*, **107**. 1546-1553.

Ropelewski, C.F. and Halpert, M.S., 1987, "Global and regional scale precipitation patterns associated with the El Niño/Southern Oscillation", *Monthly Weather Review*, **115**, 8. 1606–1626, doi: https://doi.org/10.1175/1520-0493(1987)115<1606:GARSPP>2.0.CO;2.

Satakopan, V., 1949, "A report on the rainfall studies made in connection with the unified development of the Damodar River", Delhi: Manager of Publications.

Sawant, S., Balasubramani, K. and Kumaraswamy, K., 2015, "Spatio-temporal analysis of rainfall distribution and variability in the twentieth century, over the Cauvery Basin, South India", In: Ramkumar, M., Kumaraswamy, K., Mohanraj, R., (eds), *Environmental Management of River Basin Ecosystems*. Springer Earth System Sciences. Springer, Cham. doi: https://doi.org/10.1007/978-3-319-13425-3_2.

Sharma, A. and Rajamani, V., 2001, "Weathering of charnockites and sediment production in the catchment area of the Cauvery River, southern India", *Sedimentary Geology*, **143**, 1-2. 169-184, doi: https://doi.org/10.1016/S0037-0738(01)00102-6.

Simpson, H.J., Cane, S.K. and Zebiak, S.E., 1993, "Forecasting annual discharge of River Murray, Australia, from a geophysical model of ENSO", *International Journal of Climatology*, **6**, 386–390. doi: https://doi.org/10.1002/joc.3370130407.

Sreelash, K., Mathew, M.M., Nisha, N., Arulbalaji, P., Bindu, A.G. and Sharma, R.K., 2020, "Changes in the hydrological characteristics of Cauvery River draining the eastern side of southern Western Ghats, India", *International Journal of River Basin Management.* doi: https://doi.org/10.1080/15715124.2020.1719119.

Thomas, R.G., 1993, "Rome rainfall and sunspot numbers", *Journal of Atmospheric and Terrestrial Physics*, **55**, 2. 155–164.

Vaidyanadhan, R., 1971, "Evolution of the drainage of Cauvery in South India", *Journal of Geological Society of India*, **12**, 1. 14–23, doi:https://www.geosocindia.com/index.php/jgsi/article/view/61525.

Vaithiyanathan, P., Ramanathan, A. and Subramanian, V., 1992, "Sediment transport in the Cauvery River basin: Sediment characteristics and controlling factors", *Journal of Hydrology*, **139**, 1–4. 197–210, doi: https://doi.org/10.1016/0022-1694(92)90202-7.

Valdiya, K.S., 2001, "Tectonic resurgence of the Mysore plateau and surrounding regions in cratonic Southern India", *Current Science*, **81**, 8. 1068–1089.

Ward, R., 1978, "Floods: A geographical perspective", The Macmillan Press Ltd.

Water and Power Consultancy Services (WAPCOS), 1998, Probable Maximum Precipitation (PMP) Atlas for Cauvery and Other East-Flowing River Basins: Final Report, Volume II: Maps and Tables, Central Water Commission and India Meteorological Department, New Delhi, India. Available at: CWC PMP Atlas – Cauvery and Other East-Flowing River Basins (Volume II).

Water Resources Department, Government of Tamil Nadu, 2021, Dam Rehabilitation and Improvement Project (DRIP) Phase II: Mettur Dam Environment and Social Due Diligence Report (PIC: TN12HH0005), Office of the Chief Engineer, Trichy Region. Available at: Government of Tamil Nadu – Water Resources Department.

World Meteorological Organization, 1969, "Estimation of maximum floods: Report of a working group of the Commission for Hydrometeorology". Technical Note No. 98, WMO No. 233, 208 pp. World Meteorological Organization, Geneva.

Wright, P.B., 1989, "Homogenized long-period Southern Oscillation indices". *International Journal of Climatology*, **9**. 33–54, doi: https://doi.org/10.1002/joc.3370090104.